J Therm Anal Calorim (2009) 98:347–354
DOI 10.1007/s10973-009-0313-z

Thermal stability and crystallization kinetics of ternary Se–Te–Sb semiconducting glassy alloys

Essam R. Shaaban · Ishu Kansal · M. Shapaan · José M. F. Ferreira

Received: 15 October 2008 / Accepted: 6 February 2009 / Published online: 12 August 2009

Abstract This paper presents the results of kinematical studies of glass transition and crystallization in glassy $Se_{85-x}Te_{15}Sb_x$ ($x = 2$, 4, 6 and 8) using differential scanning calorimetry (DSC). From the dependence on heating rates of, the glass transition temperatures (T_g), and temperature of crystallization (T_p) the activation energy for glass transition (E_g) and the activation energy for crystallization (E_c) are calculated and their composition dependence can be discussed in term of the average coordination number and cohesive energy. The thermal stability of $Se_{85-x}Te_{15}Sb_x$ was evaluated in terms of criterion $\Delta T = T_c - T_g$ and kinetic criteria $K(T_g)$ and $K(T_p)$. By analyzing the crystallization results, the crystallization mechanism is characterized. Two (two- and three-dimensional growth) mechanisms are working simultaneously during the amorphous–crystalline transformation of the $Se_{83}Te_{15}Sb_3$ alloy while only one (three-dimensional growth) mechanism is responsible for the crystallization process of the chalcogenides $Se_{85-x}Te_{15}Sb_x$ ($x = 4$, 6 and 8) glass. The phases at which the alloy crystallizes after the thermal process have been identified by X-ray diffraction.

E. R. Shaaban (✉)
Physics Department, Faculty of Science, Al-Azhar University, Assiut 71542, Egypt
e-mail: esam_ramadan2008@yahoo.com; esamramadan2008@gmail.com

I. Kansal · J. M. F. Ferreira
Department of Ceramics and Glass Engineering, University of Aveiro, CICECO, 3810-193 Aveiro, Portugal

M. Shapaan
Physics Department, Faculty of Science, Al-Azhar University, Cairo, Egypt

Keywords Chalcogenide · Thermal analysis · Thermal stability · Coordination number · Cohesive energy

PACS 61.43.Fs · 65.60.+a · 78.30.Ly

Introduction

Chalcogenide glasses exhibit many useful electrical properties including threshold and memory switching [1–3]. These electrical properties are influenced by the structural changes and could be related to thermally induced transitions [4, 5]. In chalcogenide glassy systems, glasses exhibiting no exothermic crystallization reaction above the glass transition temperature (T_g) show a threshold switching type [6, 7]. On the other hand, glasses exhibiting an exothermic crystallization reaction above T_g exhibit a memory type of switching. Memory switches come from the boundaries of the glass-forming regions where glasses are stable and have a tendency to crystallize when heated or cooled slowly [8–10]. Glassy alloys of chalcogen elements were the initial object of study because of their interesting semiconducting properties [11] and more recent importance in optical recording [12]. Recording materials must be stable in the amorphous state at low temperature and have a short crystallization time. Promising materials with these characteristics have been recently studied [13]. Among chalcogenide glasses, Se–Te alloys have gained much importance because of their higher photosensitivity, greater hardness, higher crystallization temperature, and smaller aging effects as compared to pure Se glass. The effect of incorporation of Sb on the electrical properties of these alloys has been studied by various workers [14–17]. In general, it is observed that the dc conductivity increases, the activation energy for dc conduction decreases, the

thermoelectric power decreases, and the photoconductive decay becomes slower on incorporation of Sb in the binary $Se_{80}Te_{20}$ alloy. In order to explain the above results it is generally assumed that the addition of Sb in the Se–Te system leads to a crosslinking of Se–Te chains which enhances the disorder in the system and hence leads to a deeper penetration of the localized state into the energy gap. This paper presents:

(a) The results of kinematical studies of glass transition and crystallization in glassy $Se_{85-x}Te_{15}Sb_x$ ($x = 2$, 4, 6 and 8) using differential scanning calorimetry (DSC). From the dependence on heating rates of (T_g), and (T_p) the activation energy for glass transition (E_g) and the activation energy for crystallization (E_c) are calculated and their composition dependence can be discussed in term of the average coordination number and cohesive energy.
(b) The evaluating of thermal stability of $Se_{85-x}Te_{15}Sb_x$ in terms of criterion $\Delta T = T_c - T_g$ and kinetic criteria $K(T_g)$ and $K(T_p)$.
(c) Characterization of the crystallization mechanism in terms of crystallization results.
(d) Identification of the phases at which the alloy crystallizes after the thermal process using X-ray diffraction.

Experimental

Bulk chalcogenide $Se_{85-x}Te_{15}Sb_x$ ($2 \leq x \leq 8$ at.%) glasses were synthesized in silica tubes from their components of high purity (99.999%). In order to avoid oxidation of the samples the tubes were evacuated to 10^{-4} Pa. The ampoules were put into a furnace at around 1,100 K for 24 h and inverted at regular intervals of time to ensure homogeneous mixing of the constituents. The ampoules were quenched in a water bath to avoid crystallization of the melts. Both the homogeneity and the compositional contents of the prepared samples were checked using energy-dispersive analysis of X-rays (EDAX). It was found that the percentage ratios of the constituent elements were close to the values taken for the starting alloys. The glassy nature of the materials was confirmed via X-ray scanning in a Philips diffractometer 1710, using Cu as target and Ni as filter ($\lambda = 1.542$ Å). The calorimetric measurements were carried out in a differential scanning calorimeter Shimadzu 50 with an accuracy of ± 0.1 K. The calorimeter was calibrated, for each heating rate, using well-known melting temperatures and melting enthalpies of zinc and indium supplied with the instrument. Twenty milligram powdered samples, crimped into aluminum pans, were scanned at continuous heating rates ($\beta = 5$, 10, 20, 30, 40 K min^{-1}). The temperatures of the glass transition, T_g, the crystallization extrapolated onset, T_{in}, and the crystallization peak, T_p, were determined with an accuracy of ± 1 K.

Results and discussion

Thermal analysis

Figure 1 shows the DSC traces for $Se_{85-x}Te_{15}Sb_x$ ($2 \leq x \leq 8$ at.%) glassy alloys at heating rate $\beta = 10$ K min^{-1}, displaying the glass transition, T_g and crystallization peak at T_p, at $\beta = 10$ K min^{-1}. The values of T_g and T_p are listed in Table 1.

The activation energy of enthalpy relaxation of the glass transition, or activation energy of glass transition, E_g, of the investigated glass can be determined using the Kissinger

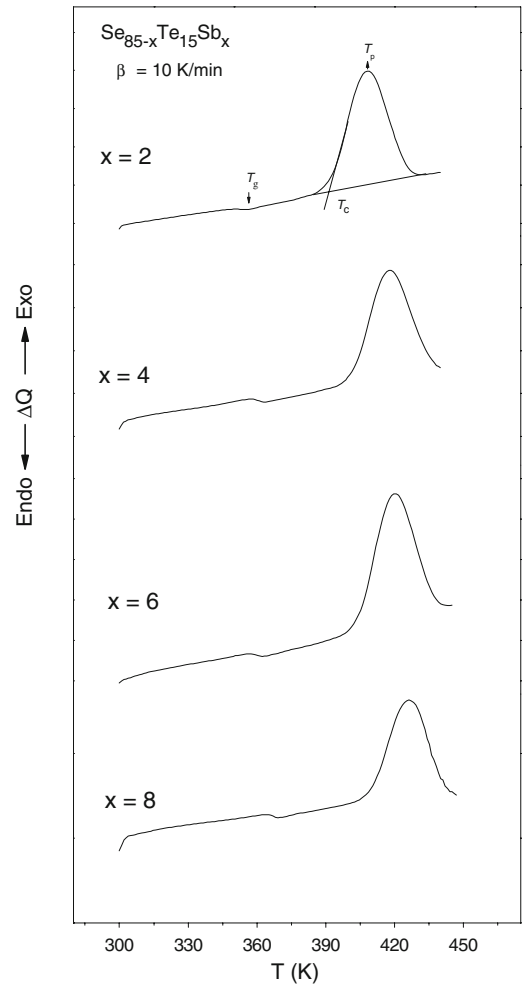

Fig. 1 Typical DSC trace of $Se_{85-x}Te_{15}Sb_x$ ($2 \leq x \leq 8$ at.%) glassy alloy at heating rate, $\beta = 10$ K min^{-1}

Table 1 The values of thermal parameters of glass transition temperature T_g, crystallization temperature, T_p and thermal stability criteria ΔT with different heating rates β and also both activation energy of glass transition, E_g and activation energy of crystallization E_c. Beside the values of average coordination number, N_c and cohesive energy, CE as a function of composition

x/at.%	N_c	B/K min^{-1}	T_g/K	E_g/kJ mol^{-1}	CE/eV	T_p/K	E_c/kJ mol^{-1}	ΔT/K
2	2.02	5	345.2	57.17	1.93	398	75.03	35.93
		10	355.3			408.1		35.89
		20	368.9			421.7		34.26
		30	374.7			427.6		34.46
		40	381			433.8		34.15
4	2.04	5	349.7	61.99	1.949	406.1	83.58	38.43
		10	361.2			417.7		36.89
		20	372.9			429.3		37.26
		30	378.7			435.2		37.46
		40	384			440.4		38.15
6	2.06	5	355.2	67.81	1.968	412.4	91.35	39.93
		10	362.8			420		42.39
		20	374.9			432.1		42.26
		30	380.7			438		42.46
		40	387			444.2		42.15
8	2.08	5	360.2	72.87	1.987	416.9	97.52	40.93
		10	369.3			426		42.89
		20	379.4			436.1		42.76
		30	385.2			442		42.96
		40	391.5			448.2		42.65

formula, which was originally derived for the crystallization process and suggested to be valid for the glass transition [18]. This formula has the following form;

$$\ln\left(T_g^2/\beta\right) = E_g/RT_g + \text{const.} \quad (1)$$

where R is the universal gas constant. Values of E_g can be estimated from the $\ln\left(T_g^2/\beta\right) - 1/T_g$ relation for different Sb contents. The subscript g denotes the values corresponding to the glass transition temperature. Figure 2 shows the verification of the linearity of $\ln\left(T_g^2/\beta\right) - 1/T_g$ relation for the studied chalcogenide. The values of the activation energy of glass transition obtained for the glass transition are listed in Table 1. Figure 3 shows the increasing trend of E_g with the increase of Sb content.

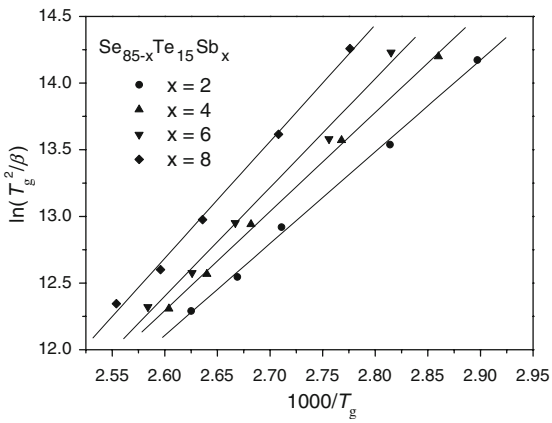

Fig. 2 Plot of $\ln\left(T_g^2/\beta\right)$ vs. $1000/T_g$ of the analyzed materials

Loffe and Regel [19] have suggested that the bonding character in the nearest neighbor region, i.e., the average coordination number N_c, characterizes the electronic properties of semiconducting materials. The average coordination number N_c in ternary compounds $Se_xTe_ySb_z$ is generalized as [20]

$$N_c = xCN(\text{Se}) + yCN(\text{Te}) + zCN(\text{Sb}) \quad (2)$$

Calculated data of N_c for the $Se_{(85-x)}Te_{15}Sb_x$ system, using the values of coordination 2, 2 and 3 for Se, Te and Sb, respectively. It can be seen that N_c increases with increasing Sb content which has higher coordination number than Te. The increase of T_g with increasing Sb content may be attributed to the marginal increases, which occur in the average coordination numbers of these alloys with increasing Sb content.

For the evaluation of activation energy for crystallization (E_c) by using the variation of T_p with β, Vázquez et al. [21] developed the proposed method by Kissinger [18] for non-isothermal analysis of devitrification as follows:

$$\ln\left[T_p^2/\beta\right] = E_c/RT_p + \ln(E/RK_0) \quad (3)$$

From the experimental data, a plot of $\ln\left[T_p^2/\beta\right]$ versus $1/T_p$ has been drawn for different compositions showing the straight regression line in Fig. 4.

The activation energy, E_c, and the frequency factor, K_0, are then evaluated by least squares fitting method of Eq. 3.

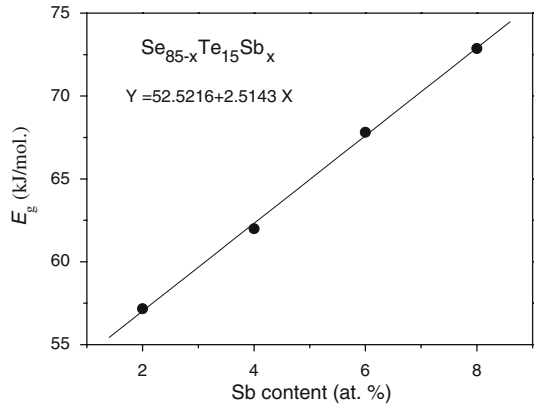

Fig. 3 Activation energy of transition E_g as a function of Sb content in $Se_{85-x}Te_{15}Sb_x$ ($2 \le x \le 8$ at.%) glassy alloy

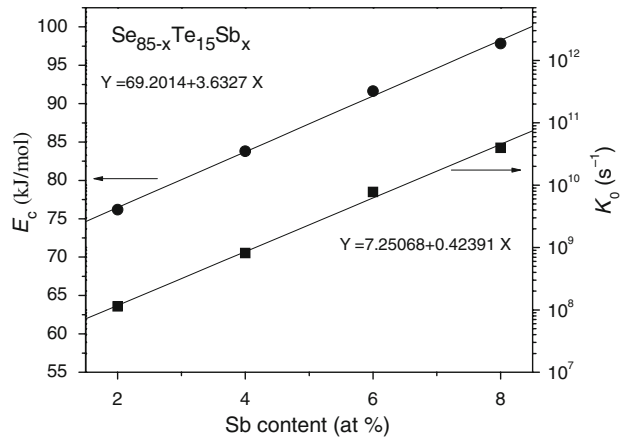

Fig. 5 The activation energy of crystallization for E_c, and frequency factor, K_0 for the of analyzed materials

Figure 5 shows the values for both E_c and K_0 as a function of Sb content. The values of the activation energy of crystallization obtained are listed in Table 1. The trend of activation energy for crystallization (E_c) can be interpreted in terms of the bond energies as follows.

The bond energies $D(A-B)$ for heteronuclear bonds have been calculated by using the relation [19]

$$D(A-B) = [D(A-A) \times D(B-B)]^{1/2} + 30(\chi_A - \chi_B)^2 \quad (4)$$

where $D(A-A)$ and $D(B-B)$ are the energies of the homonuclear bonds, χ_A and χ_B are electronegativity values for atoms involved. The electronegativity values are 2.55, 2.1 and 2.05 for Se, Te and Sb, respectively. The homonuclear bonds $D(A-A)$ are 44.04, 33 and 30.22 for Se, Te and Sb, respectively. The types of bonds expected to occur in the system under investigation are Se–Te ($D =$ 44.147 kcal mol^{-1}), Te–Sb ($D = 31.654$ kcal mol^{-1}) and Se–Sb ($D = 43.981$ kcal mol^{-1}). The assumption [22] mentioned above can be applied directly and its ambiguity

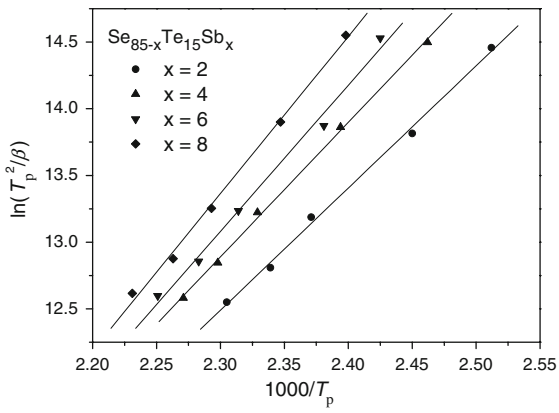

Fig. 4 Experimental plot of $\ln\left(T_p^2/\beta\right)$ vs. $1000/T_p$ for the peaks and straight regression lines for $Se_{85-x}Te_{15}Sb_x$ ($2 \le x \le 8$ at.%) glassy alloy (β in K s^{-1})

about the formal order in which the bonds are formed. After all these bonds are formed, there are still unsatisfied Se valences, which must be satisfied by the formation of Se–Se bonds. Knowing the bond energies, we can estimate the cohesive energy (CE), i.e. the stabilization energy of an infinitely large cluster of the material per atom, by summing the bond energies over all the bonds expected in the system under test. This is equivalent to assuming a simplified model consisting of non-interacting electron pair bonds highly localized between adjacent pairs of atoms. The CE of the prepared samples is evaluated from the following equation:

$$\mathrm{CE} = \sum C_i D_i / 100 \quad (5)$$

where C_i and D_i is the number of expected chemical bond and the energy of each corresponding bond. The results of (CE) are listed in Table 1. It is observed that the CE increases with increase of Sb content, meaning that the average stabilization energy increases. The increase of CE implies higher bonding strength, leads to increase in the temperature of crystallization, thus the activation energy of crystallization.

Thermal stability of chalcogenide glasses

The thermal stability, $\Delta T = T_c - T_g$ [23], is a rough measure of the glass thermal stability, where T_c is the onset temperature, so the larger differences between T_c and T_g indicating more thermal stable glasses. The values of ΔT criterion of different composition are listed in Table 1 as ΔT. It is found that the values of ΔT increase with increasing Sb content. It means that the thermal stability increases with increasing the Sb content in $Se_{85-x}Te_{15}Sb_x$ alloy system.

According to the formal theory of transformation kinetics, the kinetic parameter or the reaction rate constant

K has glass transformation temperature dependence according to the relation [24];

$$K(T) = K_0 \exp(-E_c/RT) \quad (6)$$

where E_c is the effective activation energy for crystal growth and R is the gas constant. The kinetic parameter, $K(T)$, with the above Arrhenius temperature dependence, can be introduced as a stability criteria. Surinach et al. [25] and Hu and Jiang [26] introduced two parameters,

$$K(T_g) = K_0 \exp(-E_c/RT_g) \quad (7a)$$

$$K(T_p) = K_0 \exp(-E_c/RT_p) \quad (7b)$$

The larger the values of these parameters, the greater tendency to devitrify. The values of $K(T_g)$ and $K(T_p)$ as a function of T_g and T_p for different compositions are shown in Fig. 6a and b. From the two figures, the values of $K(T_g)$ and $K(T_p)$ at a two fixed temperatures (T_{g1} and T_{g2} for Fig. 6a and T_{p1} and T_{p2} for Fig. 6b) decrease with increasing Sb content. According to the literature [26–29], the smaller the values of $K(T_g)$ and $K(T_p)$, the better should be the glass-forming ability of the material. So the data for both $K(T_g)$ and $K(T_p)$ in Fig. 6a and b indicate that the thermal stability increases with increasing Sb content.

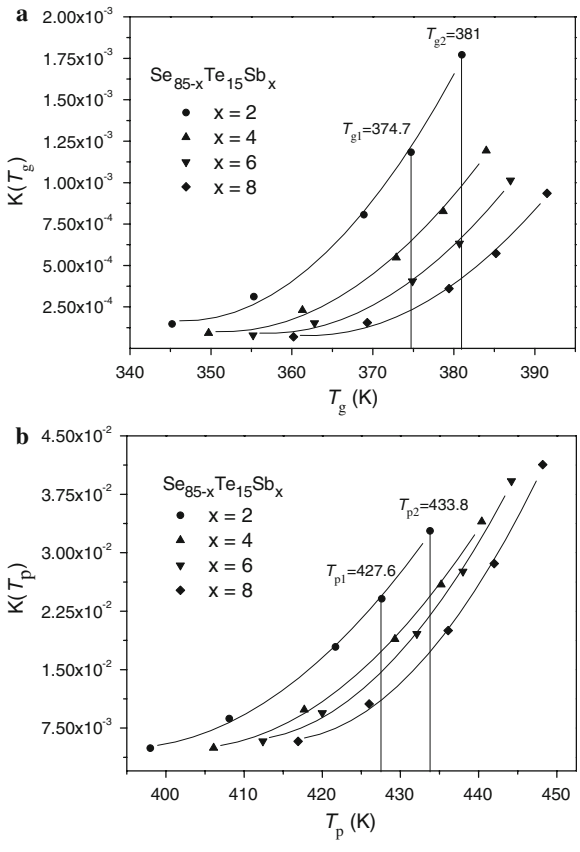

Fig. 6 **a** Plot of $K(T_g)$ vs. T_g for $Se_{85-x}Te_{15}Sb_x$ ($2 \le x \le 8$ at.%) glassy alloy. **b** Plot of $K(T_p)$ vs. T_p for $Se_{85-x}Te_{15}Sb_x$ ($2 \le x \le 8$ at.%) glassy alloy

Crystallization kinetics of glasses

Figure 7 depicts the DSC traces for the first crystallized peak of $Se_{83}Te_{15}Sb_2$ at $\beta = 10$ K min^{-1}, besides the fraction, χ, (crystallized at a given temperature T) given by $\chi = A_T/A$, where A is the total area of the exothermic peak between the temperature, T_i (the initial of crystallization) and the temperature, T_f (the full crystallization), A_T is the area between T_i and T. The graphical representation of the crystallized volume fraction, shows the typical sigmoid curve as a function of temperature for different heating rates for the first crystallization curve of $Se_{83}Te_{15}Sb_2$ (Fig. 8) based on mentioned work elsewhere [30–32].

The theoretical basis for the interpreting of the DSC results is provided by the formal theory of transformation kinetics as developed by Johnson and Mehl [33] and Avrami [34, 35]. The ratio between the ordinates of the DSC curve and the total area of the peak gives the corresponding crystallization rates that make it possible to build the curves of the exothermal peaks depicted in Fig. 9. It

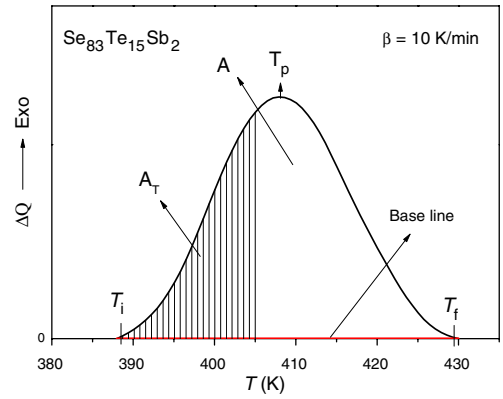

Fig. 7 DSC traces for $Se_{83}Te_{15}Sb_2$ at $\beta = 10$ K min^{-1}, the lined area A_T shows between T_i and T_f of the peak. T_i, T_f and T according to the text

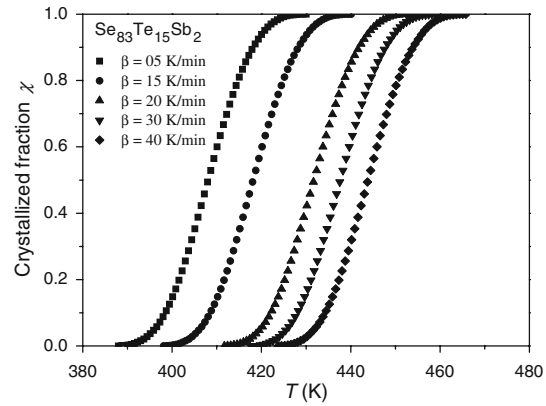

Fig. 8 Crystallized fraction, χ as a function of temperature for the peak of $Se_{83}Te_{15}Sb_2$ alloy composition at different heating rates

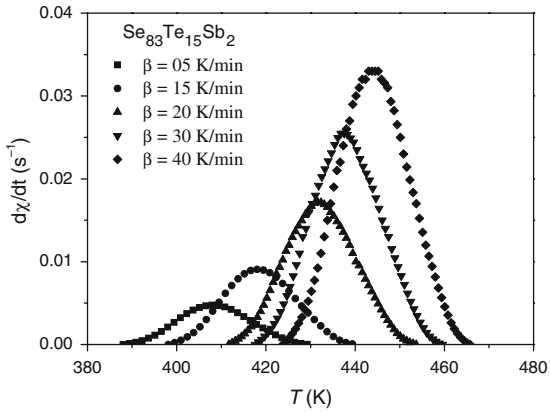

Fig. 9 Crystallization rate versus temperature of the exothermal peaks of $Se_{83}Te_{15}Sb_2$ alloy at different heating rates

was observed that the $(dx/dt)_p$ values increase as well as the heating rate, a property that has been widely discussed in the literature [36]. From the experimental values of the $(dx/dt)_p$ one can calculate the kinetic exponent n by using the following equation:

$$(d\chi/dt)_p = n(0.37\beta E_c)/RT_p^2 \quad (8)$$

Finally, the experimental data of T_p, and $(dx/dt)_p$ shown in Tables 1 and 2, respectively, along with the values of the activation energies of crystallization process, make it possible to determine, through Eq. 8, the kinetic exponent, n, using five experimental heating rates for the crystallized peaks (Table 2). The mean values, $\langle n \rangle$, are listed in Table 2. Allowing for experimental error, the value of $\langle n \rangle$ is close to 3 for all different compositions. The kinetic exponent was deduced based on the mechanism of crystallization [37]. The $\langle n \rangle$ value of the kinetic exponent of the as quenched glass is consistent with the mechanism of volume nucleation with three-dimensional growth for all different compositions [37].

Depending on the n-value [38], non-integer value of $n = 2.6$ means that two crystallization (two- and three-dimensional growth) mechanisms are working simultaneously during the amorphous–crystalline transformation of the $Se_{83}Te_{15}Sb_2$ glass while integer value of n indicates that only one (three dimensional growth) mechanism is responsible for the crystallization process of the $Se_{85-x}Te_{15}Sb_x$ ($x = 4$, 6 and 8) glass. It was supposed [39] that small antimony addition ($\sim$2 at.%) leads to cross-linking of the chains to some extent, creating a two-dimensional network. Further addition of antimony breaks the chains and forms large number of smaller chains. The natural tendency of antimony atoms is to create either a trigonal, bipyramidal or octagonal environmental with more or less covalent bonds. The Sb contributes to change the weak bonding between the Se–Te polymeric chain to relatively strong covalent bonds [39]. Three-dimensional growth responsible for crystallization of the $Se_{85-x}Te_{15}Sb_x$ ($x = 4$, 6 and 8) glass could be related to the formation of ternary crystalline phase such as Sb_2TeSe_2.

Table 2 Maximum crystallization rate ($d\chi/dt$), kinetic exponent n and average kinetic exponent $\langle n \rangle$ for $Se_{(85-x)}Te_{15}Sb_x$ ($2 \le x \le 8$ at.%) glass with different heating rates β

x/at.%	β/K min^{-1}	$(d\chi/dt) \times 10^{-3}$ s^{-1}	n	$\langle n \rangle$
2	5	4.75	2.67	2.7
	10	9.08	2.69	
	20	17.16	2.71	
	30	24.94	2.7	
	40	32.54	2.72	
4	5	5.63	3	3.02
	10	10.77	3.03	
	20	20.34	3.03	
	30	29.56	3.01	
	40	38.57	3.02	
6	5	6.34	3.18	3.16
	10	12.11	3.15	
	20	22.89	3.15	
	30	33.25	3.14	
	40	43.39	3.16	
8	5	6.69	3.22	3.19
	10	12.78	3.21	
	20	24.16	3.18	
	30	35.1	3.16	
	40	45.8	3.18	

Identification of phases using XRD

To identify the possible phases that crystallize during the thermal treatment applied to the samples, the X-ray diffraction patterns of $Se_{83}Te_{15}Sb_2$, $Se_{79}Te_{15}Sb_6$, $Se_{77}Te_{15}Sb_8$ alloys annealed at temperatures beyond the peak of crystallization temperatures with a heating rate of 10 K min^{-1} for 2 h are shown in Fig. 10. The diffractograms of the transformed material after the crystallization process suggest the presence of microcrystallites of three phases. From the JCPDS files these peaks can be identified as, (1) Antimony Tellurium Selenide, Sb_2TeSe_2 (40-1211), which crystallizes in the rhombohedral system with lattice parameters $a = b = 0.4121$ nm, $c = 2.9549$ nm, (2) Antimony, Sb (card No. 5-0562), which crystallizes in the rhombohedral structure with lattice parameters $a = b = 0.4307$ nm nm and $c = 1.1273$ nm), and (3) Selenium, Se (card No. 1-0848), which crystallizes in the hexagonal structure with lattice parameters $a = b = 0.434$ nm and $c = 0.495$ nm, while there remains also an additional amorphous phase as shown in Fig. 10. Although the same crystalline phases could be

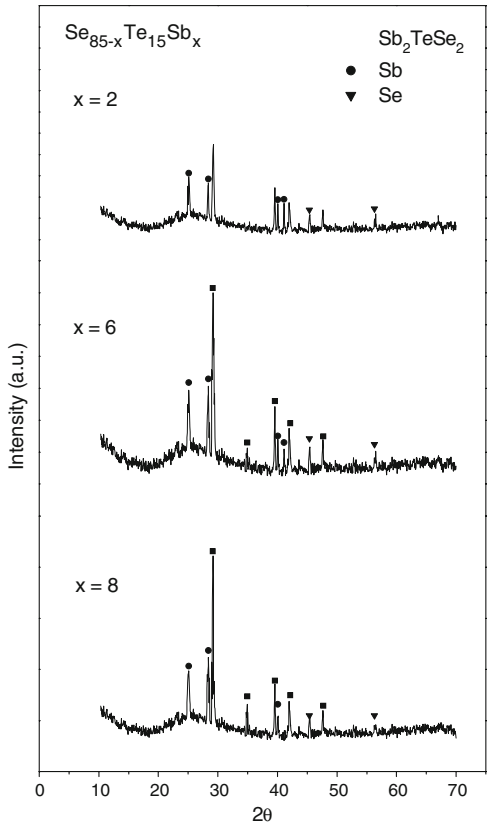

Fig. 10 XRD patterns of crystallized $Se_{85-x}Te_{15}Sb_x$ ($x = 2$, 6 and 8 at.%) alloy samples

identified in all the samples, intensity differences between the dominant peaks of each phase can be observed.

Conclusions

The results presented and discussed along this manuscript have shown that addition of Sb influences the thermal stability and crystallization kinetics, through the induced changes in phase kinetics and in the compositions of amorphous and crystalline phases. The T_g, T_p, E_g and E_c for the $Se_{85-x}Te_{15}Sb_x$ ($x = 2$, 4, 6 and 8) glassy alloys showed an increasing trend with increasing Sb. The increasing of E_g can be interpreted in terms of increasing of N_c with Sb content. And also the increasing of E_c can be interpreted in terms of increasing of CE with Sb content. The amount of Sb played a significant role in the crystallization behavior of the Se–Te chalcogenide glass, where an increase in Sb content turns the glasses more stable through increasing of ΔT and decreasing of both $K(T_g)$ and $K(T_p)$, which may be related to the increase in Sb_2TeSe_2 phase via increasing the intensity of this phase. The calculated Avrami parameters for the different crystalline phases confirm that the two (two- and three-dimensional growth) mechanisms are working simultaneously during the amorphous–crystalline transformation of the $Se_{83}Te_{15}Sb_3$ alloy while only one (three-dimensional growth) mechanism is responsible for the crystallization process of the chalcogenides $Se_{85-x}Te_{15}Sb_x$ ($x = 4$, 6 and 8) glass. The X-ray diffraction analysis of the thermal treated alloys revealed the presence of microcrystallites of Sb_2TeSe_2, Se and Sb and a remaining additional amorphous matrix.

References

1. Davis EA, Mott NF. Electronic processes in non-crystalline materials. Oxford: Clarendon; 1979.
2. Shaaban ER, Dessouky MT and Abousehly AM. Glass forming tendency in ternary $Ge_xAs_{20}Te_{80-x}$ glasses examined using differential scanning calorimetry. J Phys Condens Matter. 2007;19: 096212 (11 pp).
3. López FA, Ramirez MC, Pons JA, López-Delgado A, Alguacil FJ. Kinetic study of the thermal decomposition of low-grade nickeliferous laterite ores. J Therm Anal Calorim. 2008;94:517–22.
4. Novita DI, Boolchand P. Fast-ion conduction and flexibility of glassy networks. Phys Rev Lett. 2007;98:195501.
5. Malta L, Medeiros M. Thermal analysis and structural characterization of $Bi_4V_{2-x}Ba_xO_{11-1.5x}$ ($0.02 \leq x \leq 0.50$). J Therm Anal Calorim. 2007;87:883–6.
6. Živković D, Milosavljević A, Mitovski A, Marjanović B. Comparative thermodynamic study and characterization of ternary Ag–In–Sn alloys. J Therm Anal Calorim. 2007;89:137–42.
7. Phillips JC, Thorpe MF. Constraint theory, vector percolation and glass formation. Solid State Commun. 1985;53:699–702.
8. Savage JA. Glass-forming region and DTA survey of some glasses in the Si-Ge-As-Te threshold switching glass system. J Mater Sci. 1972;7:64–7.
9. Sánchez-Jiménez PE, Criado JM, Pérez-Maqueda LA. Kissinger kinetic analysis of data obtained under different heating schedules. J Therm Anal Calorim. 2008;94:427–32.
10. Moss SC, Deneufville JP. Thermal crystallization of selected thin films of Te-based memory glasses. Mater Res Bull. 1972;79:423–42.
11. Tanaka K, Osaka Y, Sugi M, Iizima S, Kikuchi M. Kinetics of growth of conductive filament in As–Te–Ge glasses. J Non-Cryst Solids. 1973;12:100–14.
12. Sugiyama Y, Chiba R, Fugimori S, Funakoski N. Crystallization process of In–Te alloy films for optical recording. J Non-Cryst Solids. 1990;122:83–9.
13. Maeda Y, Andoh H, Ikuta I, Magai M, Katoh Y, Minemura H, et al. Single-beam overwriting with melt-erasing process in an InSbTe phase-change optical disk. Appl Phys Lett. 1989;54:893–5.
14. Kasap SO, Juhasz C. Kinematical transformations in amorphous selenium alloys used in xerography. J Mater Sci. 1986;21:1329–40.
15. Tripathi SK, Kumar A. Steady state and transient photoconductivity in amorphous thin films of $Se_{0.8}Te_{0.2}$. J Electron Mater. 1988;17:45–51.
16. Arora R, Kumar A. Dielectric relaxation in glassy Se and $Se_{100-x}Te_x$ alloys. Phys Stat Sol A. 1989;115:307–14.
17. Agarwal P, Goel S, Rai JSP, Kumar A. Calorimetric studies in glassy $Se_{80-x}Te_{20}In_x$. Phys Stat Sol A. 1991;127:363–9.
18. Kissinger HE. Reaction kinetics in differential thermal analysis. Anal Chem. 1957;29(11):1702–6.
19. Loffe AF, Regel AR. Non-crystalline, amorphous and liquid electronic semiconductors. Prog Semicond. 1960;4:239.

20. Shaaban ER. Calculation of optical constant of amorphous germanium arsenoselenide wedge-shaped thin films from their shrunk transmittance and reflectance spectra. Phil Mag. 2008;88 (5):781–94.
21. Vazquez J, Lopez-Alemany PL, Villares P, Jimenez-Garay R. Generalization of the Avrami equation for the analysis of non-isothermal transformation kinetics. Application to the crystallization of the $Cu_{0.20}As_{0.30}Se_{0.50}$ alloy. J Phys Chem Solids. 2000;61: 493–500.
22. Ovshinsky SR. Principles and applications of amorphicity, structural change, and optical information encoding. J Phys 1981;C4/ 42:1095–104.
23. Chen HS. A method for evaluating viscosities of metallic glasses from the rates of thermal transformations. J Non-Cryst Solids. 1978; 27:257–63.
24. Shaaban ER, Shapaan M, Saddeek YB. Structural and thermal stability criteria of Bi_2O_3–B_2O_3 glasses. J Phys Condens Matter. 2008;20:155108.
25. Hu L, Jiang Z. New criterion for crystallisation of glass. J Chin Ceram Soc. 1990;18:315–21.
26. Surinach S, Baro MD, Clavaguera-Mora MT, et al. Glass formation and crystallization in the $GeSe_2$–Sb_2Te_3 system. J Mater Sci. 1984;19:3005–12.
27. Vàzquez J, López-Alemany PL, Villares P, Jiménez-Garay R. Evaluation of the glass forming ability of some alloys in the Sb–As–Se system by differential scanning calorimetry. J Alloy Compd. 2003;354:153–8.
28. Shaaban ER, Dessouky MT, Abousehly AM. The effect of Bi content on the thermal stability and crystallization of Se–Te chalcogenide glass. Phil Mag. 2008;88(7):1099–112.
29. Shaaban ER. Physica B. Non-isothermal crystallization kinetic studies on a ternary, $Sb_{0.14}As_{0.38}Se_{0.48}$ chalcogenide semi-conducting glass. 2006;373:211–6.
30. Wagner C, Villanes P, Vázquez J, Jirnenex-Caray R. Some methods for kinetic studies of non-isothermal crystallization in $Sn_{0.08}As_{0.26}Se_{0.66}$ alloy. Mater Lett. 1993;19:370–5.
31. Goel A, Shaaban ER, Ribeiro MJ, Melo FCL, Ferreira JMF. Influence of NiO on the crystallization kinetics of near stoichiometric cordierite glasses nucleated with TiO_2. J Phys Condens Matter. 2007;19:386231–45.
32. Johnson WA, Mehl RF. Reaction kinetics in processes of nucleation and growth. Trans Am Inst Min Met Eng. 1939;135: 416–58.
33. Avrami M. Kinetics of phase change. II transformation-time relations for random distribution of nuclei. J Chem Phys. 1940;8: 212–24.
34. Avrami M. Granulation, phase change, and microstructure kinetics of phase change. III. J Chem Phys. 1941;9:177–84.
35. Gao YQ, Wang W, Zheng FQ, Liu X. On the crystallization kinetics of $Pd_{80}B_4Si_{16}$ glass. J Non-Cryst Solids. 1986;81:135–9.
36. Matusita K, Saka S. Kinetic study of crystallization of glass by differential thermal analysis—criterion on application of Kissinger plot. J Non-Cryst Solids. 1980;38–39:741–6.
37. Yinnon H, Uhlmann DR. Applications of thermoanalytical techniques to the study of crystallization kinetics in glass-forming liquids, part I: theory. J Non-Cryst Solids. 1983;54:253–75.
38. Mehra RM, Gurinder A, Ganjoo A, Singh R, Mathur PC. Effect of antimony doping on the transport properties of the glassy $Se_{80-x}Te_{20}Sb_x$ system. Phys Stat Sol A. 1991;124:K51–3.
39. Mehdi M, Brun G, Tedenac JC. Crystallization kinetics of bulk amorphous $(Se_{65}Te_{35})_{100-x}Sb_x$. J Mater Sci. 1995;30:5259–62.